ROYAL SOCIETY
OF CHEMISTRY

PAPER

Check for updates

A hybrid 3D-printed aspirin-laden liposome composite scaffold for bone tissue engineering†

Yan Li,[ab] Yanjie Bai,*[c] Jijia Pan,[a] Hui Wang,[d] Hongming Li,[e] Xiao Xu,[b] Xiaoming Fu,[b] Rui Shi,[b] Zuyuan Luo,[a] Yongliang Li,[b] Qian Li,[a] Jerry Y. H. Fuh[d] and Shicheng Wei ✱[ab]

Bone defects are some of the most difficult injuries to treat in clinical medicine. Evidence from cellular and animal studies suggests that aspirin exhibits protective effects on bone by promoting both the survival of osteoblast precursor stem cells and osteoblast differentiation. However, acquired resistance to aspirin and its cytotoxicity significantly limit its therapeutic application. Controlled release systems have been confirmed to promote the efficacy of certain drugs for bone regeneration. Additionally, the controlled release of a high dose of drug allows for lower dosing over an extended period. In this way, nano-liposomal encapsulation of aspirin can be used to reduce the cytotoxicity of the overall dose. Using a series of osteogenic experiments, this study found that an aspirin-laden liposome delivery system (Asp@Lipo) obviously promoted osteogenesis and immunomodulation of human mesenchymal stem cells (hMSCs). We also studied the *in vitro* capacity of polycaprolactone (PCL)-based bioactive composite (PCL-Asp@Lipo) scaffolds to facilitate cell proliferation and osteoblast differentiation. Compared to a common scaffold, ALP assays, immunofluorescence and calcium mineralisation studies revealed that the PCL-Asp@Lipo scaffolds enhanced the osteogenic differentiation of hMSCs. Subsequently, along with the cells, PCL and PCL-Asp@Lipo scaffolds were both implanted subcutaneously into nude mice for estimation of osteo-inductivity after 6 weeks, the PCL-Asp@Lipo composite scaffold exhibited more osteogenic activity than the bare PCL scaffold. This approach has potential applications in bone tissue repair and regenerative medicine.

1. Introduction

The reconstruction of damaged bone tissue related to congenital abnormalities, trauma and cancer is an especially important challenge for bone tissue engineering (BTE).[1,2] Guiding stem cell differentiation to yield a specific cell type is crucial in any cell therapy. If not properly controlled, stem cells are likely to differentiate into unneeded cells, or even worse, lead to tumours.[3,4] A safe and advanced technique that can promote the reorganisation of functional tissue by controlling stem cell

[a] *Laboratory of Biomaterials and Regenerative Medicine, Academy for Advanced Interdisciplinary Studies, Peking University, Beijing 100871, China. E-mail: sc-wei@pku.edu.cn; Fax: +86 10 82195771; Tel: +86 10 82195771*

[b] *Central Laboratory and Department of Oral and Maxillofacial Surgery School and Hospital of Stomatology, Peking University, Beijing 100081, China*

[c] *Department of Stomatology, Peking University Third Hospital, Peking University, Beijing 100191, China. E-mail: yanjiebai@126.com; Fax: +86 01082266889; Tel: +86 01082266889*

[d] *National University of Singapore Suzhou Research Institute, Suzhou 215123, China*

[e] *College of Life Science, Mudanjiang Normal University, Mudanjiang 157011, China*

† Electronic supplementary information (ESI) available. See DOI: 10.1039/c8tb02756k

differentiation is urgently needed.[5] Aspirin, the first nonsteroidal anti-inflammatory drug (NSAID), was synthesised in 1899 and remains the most widely used drug in the world,[6] with approximately 36% of adults in the United States taking aspirin as a preventative measure against cardiovascular disease.[7] Aspirin is used therapeutically for a variety of ailments including pain, colorectal cancer, diabetes, cardiovascular diseases and inflammation and thromboprophylaxis in orthopaedic surgeries.[8,9] However, aspirin causes long-lasting functional deficit in platelets and a prolongation of bleeding time is clinically detectable.[10] Despite the extensive use of aspirin, high-dose aspirin therapies can be cytotoxic, resulting most commonly in gastrointestinal bleeding.[11] Additionally, resistance and nonresponse to aspirin can result in incomplete inhibition of platelet function,[10] inadequately low doses and/or concurrently administered proton pump inhibitors, leading to reduced absorption of active aspirin.[9,12–14] In a related study, Yamaza showed that aspirin increased the bone-forming capacity of immunocompromised rats that had received transplanted bone marrow mesenchymal stem cells.[15] Further studies have shown that aspirin facilitates the migration and homing of stem cells.[16] Aspirin use is particularly prevalent among elderly individuals susceptible to bone loss.[17] Regrettably, the common side-effects of aspirin can lead to gastrointestinal diseases, which limits its long-term use.[18]

This journal is © The Royal Society of Chemistry 2019

J. Mater. Chem. B, 2019, 7, 619–629 | 619

However, despite its limitations, aspirin continues to have a positive role in the regulation of bone disorders, and is expected to do so for years to come.[19] Aspirin microencapsulation with controlled release and delivery would allow for increased drug half-lives, improved drug absorption and more precise targeting for tissue regeneration. This strategy is being considered for high-dose aspirin therapies.

Considerable efforts have been applied to the creation of new functional materials for use as drug delivery vehicles. These include inorganic and organic polymers, and various composites thereof. Liposomes were discovered by Bangham in 1964 and liposomal nanotechnology has evolved significantly since then.[20] They are commonly found in commercially successful delivery vectors[21] because they are relatively simple, biocompatible, biodegradable and scalable materials. They also boast low cytotoxicity, do not activate the immune system and can be applied to load hydrophobic and hydrophilic drugs.[12–14] Moreover, liposomes have wide applications in the cosmetic,[22] food,[23] pharmaceutical,[24] and textile[25] industries.

Biomaterials have an active role in drug delivery systems and can be used to enhance the *in vivo* activity of a growth factor or drug through, for example, controlled release. Liposomes, as a drug delivery system, can deliver drugs to the site of action directly and maintain their levels for long periods, along with reducing the cytotoxicity of certain drugs and improving their therapeutic activity.[26,27] Thus, we hypothesised that the incorporation of bioactive aspirin into a liposome-based delivery system would exert positive effects on the osteoblast differentiation of stem cells.

Bone defects larger than a critical size may surpass the self-healing ability of bone, requiring clinical intervention that often includes grafting a cell support platform or scaffold over the defect area. One promising approach is the fabrication of three-dimensional (3D)-printed scaffolds.[28] These scaffolds can serve as temporary matrices for supporting cell growth or direct cell differentiation *via* mechano-induction, ultimately resulting in bone remodelling. However, in BTE, the majority of single-polymer scaffolds used in clinical trials do not show osteo-induction.[5,29] Hence, BTE biomaterials are increasingly involving composites that leverage and combine the strengths of individual materials. For example, the surface of the scaffold can be functionalised with drugs to yield a BTE drug delivery system.

This study focused on the synthesis of aspirin-laden liposomes and used a series of *in vitro* experiments to demonstrate their efficacy as an osteo-inductive drug delivery system. Polycaprolactone (PCL) scaffolds are conducive to bone tissue regeneration because of their biocompatibility, controllable degradability and ease of handling. However, the surface of PCL scaffolds has poor bioactivity and does not facilitate cell differentiation to a desired cell type or lineage.[30] A hybrid 3D scaffold with an incorporated drug delivery system would overcome many of the disadvantages of synthetic biopolymer scaffolds in BTE. This study demonstrated that PCL-based bioactive composite scaffolds (PCL-Asp@Lipo) promoted both *in vitro* and *in vivo* osteoblast differentiation of hMSCs (Fig. 1). We also assessed the osteo-inductive potential of these bioactive composite scaffolds in a subcutaneous rat model. Our results suggest that PCL-Asp@Lipo scaffolds are a safe and promising material for use in BTE applications.

2. Experimental

2.1. Materials

The 3D-printed PCL scaffolds were provided by the National University of Singapore Suzhou Research Institute (NUSRI). Dopamine was obtained from Sigma-Aldrich (USA). 1,2-Dipalmitoyl-*sn*-glycero-3-phosphocholine (DPPC) was provided by Tokyo Chemical Industry (Japan). Tris(hydroxymethyl)aminomethane hydrochloride (Tris–HCl) was provided by Sinopharm Chemical Reagent Co. Ltd (China). Cholesterol was obtained from Sigma-Aldrich. L-α-Phosphatidylethanolamine-*N*-(lissamine rhodamine B sulfonyl) (ammonium salt) (egg-transphosphatidylated, chicken) (PE-Rho) was obtained from Avanti Polar Lipids (USA). 1,2-Distearoyl-*sn*-glycero-3-phosphoethanolamine-*N*-[amino(polyethylene glycol)-2000] (DSPE-PEG-NH$_2$) was provided by Ruixi Biological Technology Co. Ltd (China). All reagents were of analytical grade.

2.2. Fabrication and characterisation of aspirin-laden liposomes

Aspirin-laden liposomes were fabricated by a film dispersion method as described previously.[31–33] Briefly, aspirin and lipids were dissolved in a mixture of methanol and chloroform (1 : 1, v/v) in a round-bottomed flask, and predetermined proportions of
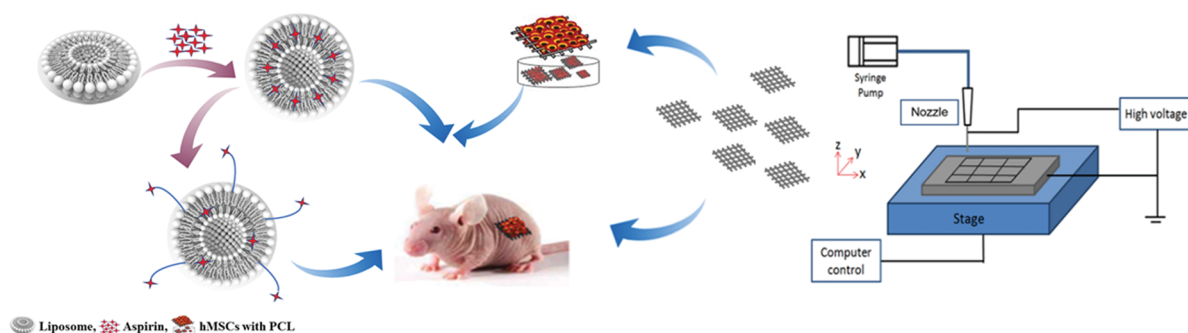

Fig. 1 Schematic illustration of hybrid 3D-printed aspirin-laden liposome composite scaffold.

aspirin were prepared at various mixed volume ratios with the methanol and chloroform mixture. Then, a rotary vacuum evaporator was used to remove the methanol and chloroform, and the lipid film was hydrated in phosphate-buffered saline (PBS). After sonication in a water bath for 5 min ($T = 47\ ^{\circ}$C), the aspirin-laden liposomes were obtained. Extrusion through porous polycarbonate membranes (Millipore, USA) with pore sizes of 450, 220 and 100 nm ensured that the final liposomes were uniform. Then, aspirin-laden liposomes were dialysed against PBS at 4 $^{\circ}$C. The polydispersity index (PDI), particle size and zeta potential were measured as previously reported.[31] The encapsulation efficiency (EE) of aspirin was calculated as EE $= (W_1/W_2) \times 100\%$, where W_1 is the measured amount of aspirin in a liposome suspension after dialysing overnight against PBS, and W_2 is the measured amount of aspirin in the initial liposome suspension.

2.3. Synthesis and characterisation of surface-adsorbed aspirin-laden liposomes

Dopamine solution (2 mL; 2 mg mL^{-1}, pH = 8.5) was added into the cell culture plates (PS) and gently shaken at 37 $^{\circ}$C overnight. To remove polydopamine (PDA) particles, the PDA-decorated PS surfaces (PS-PDA) were ultrasonically cleaned in sterile distilled water for 5 min, followed by immersing in a solution containing aspirin-laden liposomes for 24 h at 37 $^{\circ}$C. The resulting surfaces, bearing adsorbed aspirin liposomes, were washed gently with PBS three times. The aspirin liposomes immobilised on the PCL scaffolds were prepared by the same method.

PS with and without PDA/Lipo modifications was characterised by confocal laser scanning microscopy (CLSM; Carl Zeiss, Germany), X-ray photoelectron spectroscopy (XPS; Kratos Analytical, UK) and transmission electron microscopy (TEM; H-9000; Hitachi, Japan). The binding of PE-Rho-loaded liposomes to pristine (PS) substrates was analysed by CLSM. The presence of liposomes and alteration of chemical composition were determined by XPS. The morphology of the liposomes with or without aspirin immobilised on the surface was analysed using TEM. Meantime, changes in the PCL scaffolds' morphologies, with or without liposome immobilisation, were characterised by field-emission scanning electron microscopy (FE-SEM; S-4800; Hitachi).

2.4. *In vitro* release of aspirin

The release profiles of aspirin from aspirin-laden liposomes, with or without immobilisation on the substrate, were determined by dialysis of the release medium (PBS). Firstly, 1 mL of aspirin-laden liposome was suspended in a dialysis bag (MW cut-off 8000–14 000 Da; Union Carbide, USA) and immersed in 50 mL of PBS. Similarly, aspirin liposome-immobilised PS and PCL substrates were immersed in the PBS release medium. The dialysis system was maintained at 37 $^{\circ}$C and shaken at 60 rpm at scheduled times. At each sampling time, a 100 μL aliquot of release medium was collected from the dialysis system. The aspirin concentration of the aliquot was analysed using a microplate reader (Model 680; Bio-Rad, Canada) by measuring the solution absorbance at 277 nm.

2.5. Cytocompatibility

2.5.1. Cell culture. Human mesenchymal stem cells (hMSCs; ATCC, USA) were cultured in normal growth media containing Dulbecco's modified Eagle's medium (DMEM) (Gibco, USA), 10% foetal bovine serum (FBS) (Gibco), 1% penicillin and streptomycin (Amresco, USA) at 37 $^{\circ}$C in 5% CO_2.

2.5.2. Cell proliferation. Cell proliferation on different samples was evaluated using a Cell Counting Assay Kit-8 (CCK-8; Dojindo Laboratories, Japan) following the manufacturer's protocol. Briefly, at 1, 3 and 5 days, the cells were incubated in a 1 : 10 (v/v) solution of CCK-8 in culture medium and incubated at 37 $^{\circ}$C for 2 h. Supernatant (100 μL) was transferred from each well for measurement of the optical density (OD) at 450 nm using a microplate reader. Three parallel specimens for each set of experimental conditions provided averages and standard deviations for data analysis.

2.6. ELISA assays

The inflammatory cell model was prepared as previously reported.[2,34] The expression levels of tumour necrosis factor-α (TNF-α), interferon-γ (IFN-γ), receptor activator of nuclear factor-κB ligand (RANKL) and osteoprotegerin (OPG) were detected using an ELISA kit (Qisong Biological Technology, China) according to the manufacturer's instructions. Absorbance data were obtained from each well at 450 nm.

2.7. *In vitro* osteoblast bioactivity of hMSCs

2.7.1. Aspirin-laden liposome-induced osteoblast bioactivity on pristine (PS) substrates. Human mesenchymal stem cells were seeded onto substrates bearing either empty or aspirin-laden liposomes. The control groups were hMSCs on PS substrates (negative control) and hMSCs that had been treated with aspirin (free state, 75 μg mL^{-1}) on PS substrates (positive control). Osteo-inductive media was prepared by supplementing ascorbic acid (50 μg mL^{-1}; Sigma), dexamethasone (100 nM; Sigma) and β-glycerophosphate (10 mM; Sigma) to the normal growth medium.

2.7.2. Gene analysis. The hMSCs were lysed with TRIzol reagent (Invitrogen, USA) and a RevertAid First Strand cDNA Synthesis Kit (Fisher Scientific, USA) was used to convert them into cDNA. Qualitative real-time polymerase chain reaction (qPCR) was conducted using an ABI 7500 RT-PCR instrument (Applied Biosystems, USA) using SYBR Green dye (Roche, USA) in triplicate; β-actin mRNA was used as an internal control. The primers used are listed in Table S1 (ESI†). The comparative CT ($2^{-\Delta\Delta CT}$) method was applied to evaluate gene expression differences between the groups.

2.7.3. Alkaline phosphatase (ALP) assays. The ALP activity of hMSCs on different samples was assessed using an ALP assay reagent kit (NJJC-BIO, China). Cells were resuspended in Triton X-100 (1%) for 1 h, followed by collection and centrifugation of the cell-lysis solution (4 $^{\circ}$C, 13 000 rpm) for 20 min to remove cell debris. Then, the supernatant was transferred for ALP determination following the manufacturer's instructions. The ALP activity value was normalised by the total protein content,

which was determined using a bicinchoninic acid (BCA) protein assay kit (Fisher Scientific). Meanwhile, the *in situ* enzyme-histochemistry staining for ALP was visualised by a BCIP/NBT ALP colour development kit (Beyotime, China) according to the manufacturer's instructions.

2.7.4. Alizarin Red S (ARS) staining. To detect calcium mineralisation, hMSCs were induced for 21 days, fixed with 4% paraformaldehyde, stained with Alizarin Red S (2%; Sigma-Aldrich) and the samples were observed by inverted phase contrast microscopy (Eclipse TE2000-U; Nikon, Japan). To determine calcium content quantitatively, stained samples were destained with 1% hexadecylpyridinium chloride (Sigma-Aldrich) for 24 h. The calcium concentration was evaluated by measuring the absorbance at 560 nm using a multiplate reader.

2.7.5. Immunofluorescence (IF) staining. Osteogenic differentiation of hMSCs was determined on day 21 by immunofluorescence (IF) analyses. Firstly, hMSCs were fixed with paraformaldehyde (4%) for 10 min, permeabilised with Triton X-100 (0.1%) for 20 min and blocked with bovine serum albumin (BSA) (3%; Sigma) in PBS for 1 h. Next, cells were incubated with primary antibodies at 4 °C overnight. The primary antibodies used were mouse anti-osteocalcin (anti-OCN) at a 1:100 dilution (Abcam, UK) and rabbit anti-osteopontin (anti-OPN) at a 1:100 dilution (Abcam). Then, they were washed twice with PBS and incubated with secondary antibodies for 1 h in the dark. The secondary antibodies used were TRITC-543 goat antimouse (1:500; Cell Signaling Technology, USA) and FITC-488 goat antirabbit (1:500, Cell Signaling Technology). Finally, DAPI was used for staining cell nuclei and fluorescence signals were visualised by CLSM immediately.

2.8. Osteogenic differentiation on PCL-based composite scaffolds

The PCL scaffolds were produced as follows: sufficient PCL solution was added into the reservoir fitted with a 200 μm inner diameter stainless steel nozzle. A substrate was placed on the XYZ stage; the distance between nozzle and substrate was 2 mm. Solution supplement was delivered at 15 μL min^{-1} by a stepping motor and 2.4 kV was applied between the nozzle and substrate. Additionally, liposome-decorated PCL substrates were prepared as described above (Section 2.3). The proliferation and osteogenic differentiation of hMSCs cultured on aspirin-laden liposome-decorated PCL substrates were investigated *in vitro*. The ALP activity was evaluated at 7 and 14 days. Additionally, calcium mineralisation was assessed by ARS staining and IF analysis at day 21; hMSCs on pristine and blank liposome-decorated PCL substrates were used as controls, respectively.

2.9. Subcutaneous implantation

Subcutaneous implantation experiments were performed on male BALB/c-nu mice (6 weeks, 20 ± 2 g). All animal procedures described in this study were approved by the Animal Care and Use Committee of Peking University. Before implantation, PCL and PCL-Asp@Lipo composite scaffolds were co-cultured *in vitro* with hMSCs for 7 days. Then, mice were anaesthetised by intraperitoneal injection of sodium pentobarbital (1%) to induce general anaesthesia. Next, one skin incision was created on the dorsal surface of each mouse. Each mouse had six subcutaneous implants containing 1.8×10^6 cells *in vivo* for 6 weeks.

2.10. Micro-CT and histological analysis

The mice were euthanised (n = 6 for each group) at 6 weeks post-implantation and the implants were retrieved and fixed in neutral formalin (10%; Solarbio, China) for further analyses. For observation of the total bone volume formed on the PCL and PCL-Asp@Lipo composite scaffolds, the implants were imaged (60 kV, 0.22 mA, 60 s) using a high resolution micro-CT specimen scanner (Inveon MM CT; Siemens, Germany). Additionally, the bone volume fraction (bone volume/total volume, BV/TV) was calculated using Inveon Research Workplace software (Siemens). A threshold (1000–4500 mg HA cc^{-1}) was determined subjectively from the reconstructed images to partition mineralised tissue from fluid and soft tissues. Afterwards, the specimens were embedded in paraffin and sectioned (5 μm) for ARS, immunohistochemistry (IHC) and IF staining. For ARS staining, the slices were first subjected to dewaxing hydration, then incubated with ARS solution stain for 30 min at room temperature (RT). Dehydration, transparency rendering and sealing with neutral resin followed. Finally, the slices were imaged using a light microscope. For IHC staining, after washing with PBS, the slices were incubated with primary antibody against OPN (rabbit monoclonal, 1:200) at 4 °C overnight. Additionally, slices were exposed to horse radish peroxidase (HRP)-conjugated secondary antibody (goat antirabbit, 1:200) for 1 h at RT. Finally, the 3-3′diaminobenzidine (DAB) peroxidase substrate system was used for colour development and the images were captured under a light microscope. The IF staining method was similar to that for IHC; primary antibodies against collagen type 1 (Col1a1; ab90395) and RUNX-2 (ab76956) were obtained from Abcam and the images were visualised using CLSM.

2.11. Cytokine levels in subcutaneous implantation

The specimens (PCL and PCL-Asp@Lipo) were harvested at 3 days after transplantation into the C57BL/6 mouse model. The inflammatory factors (TNF-α and IFN-γ) were measured with a commercial ELISA kit in the subcutaneous implantation tissues following the manufacturer's instructions.

2.12. Statistical analysis

Data are shown as the mean ± standard deviation. All experiments were conducted with at least three biological replicates. Statistical comparison among groups was performed by one-way ANOVA and Tukey's *post hoc* tests for multiple comparisons. The results are considered significant at P-values less than 0.05.

3. Results and discussion

3.1. Fabrication and characterisation of Asp@Lipo

Liposomes are defined as phospholipid vesicles including one or more concentric lipid bilayers surrounding discrete aqueous

622 | *J. Mater. Chem. B,* 2019, **7**, 619–629

This journal is © The Royal Society of Chemistry 2019

Table 1 Characterization of the aspirin liposomes

Liposomes	Particle size (nm)	Polydensity index	ζ potential (mV)
Blank liposomes	194.5 ± 2.81	0.218 ± 0.007	0.292 ± 0.024
Aspirin liposomes	198.6 ± 1.37	0.183 ± 0.034	0.366 ± 0.002

spaces. It has been demonstrated that liposomes can provide good drug loading for both hydrophilic and lipophilic drugs, as well as enhance drug solubility and stability.[35–38] In 1971, the first report was published concerning liposomal encapsulation of a therapeutic agent.[39] Then, a novel polyelectrolyte-stabilised liposome was reported for doxorubicin; this showed a 5.9-fold improvement in oral bioavailability of doxorubicin compared to the free drug.[40] Liposomes have promoted therapies for a series of biomedical applications by stabilising therapeutic compounds, and have become the most widely used and well-investigated nanocarriers for targeted drug delivery.[41]

Table 1 lists the liposome size, PDI and ζ-potentials. The size distribution of liposomes was highly monodisperse, varying from 194.5 ± 2.81 nm for empty liposomes to 198.6 ± 1.37 nm for aspirin-laden liposomes, with low PDI (approximately 0.2) and almost neutral ζ-potentials. The TEM micrographs in Fig. S1a (ESI†) show that the liposomes maintained their size and primarily round morphologies after aspirin loading, *i.e.* loading with aspirin did not significantly alter the overall shape or size of the liposomes. To quantify the amount of liposome-encapsulated aspirin, ODs were measured before and after aspirin loading. Fig. S1b and c (ESI†) show that the EEs at three different aspirin concentrations (50, 75 and 100 μg mL^{-1})

were ∼99.46%, ∼99.89% and ∼96.81%, respectively. The optimal aspirin concentration for encapsulation (75 μg mL^{-1}) was selected for further experiments.

3.2. Synthesis and characterisation of the Asp@Lipo-decorated substrate

Dopamine molecules can self-polymerise and then form a PDA structure under weakly alkaline conditions (pH = 8.5).[32] This polymer offers many catecholamine moieties as amine group binders. Through the amine–catechol reaction, aspirin-laden liposomes could be grafted to the PDA layer in this study, to produce liposome-decorated surfaces. The resulting aspirin-laden liposome-decorated PS surfaces were examined using CLSM and XPS to characterise changes in the morphology and chemical composition after the surface decoration.

The representative fluorescence images in Fig. 2a show that liposomes were uniformly distributed over the substrate surface. In contrast, no fluorescence was observed from PS samples that had not been prepared with decoration of liposomes. This suggests only slight autofluorescence and a lack of immobilised liposomes on the PS surfaces. The XPS spectra in Fig. 2b show the differences in surface chemistry of the PDA-decorated PS substrates (PS-PDA) after liposome grafting. The predominant peak in the XPS spectrum of PS-PDA was N (1s). The presence of phosphorus peaks (P (2s) and P (2p)) indicate that immobilisation of the lipids on the PS-PDA surfaces was successful. Both the fluorescence and XPS data indicate that liposomes were grafted successfully on the PS-PDA surfaces. Also, SEM images of the PCL surfaces (Fig. S2, ESI†) revealed a surface morphology of the PCL-Asp@Lipo scaffold that was
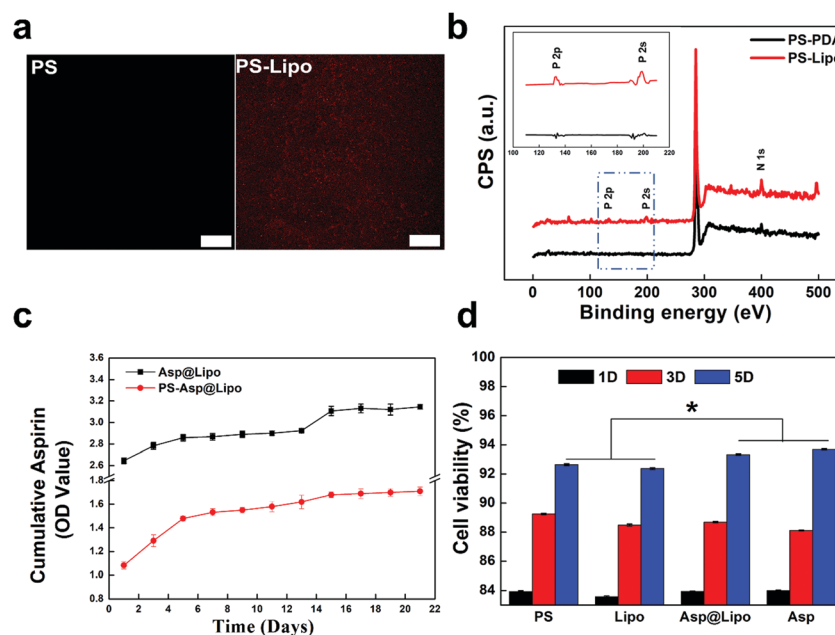

Fig. 2 Surface characterization of the substrates (pristine and functionalized PS) and aspirin release and hMSCs proliferative activity as a function of time. (a) Fluorescence micrograph of Rho-PE-labeled liposomes immobilized on the surface of PS substrates. The scale bar represents 50 μm. (b) XPS survey scan spectra. (c) *In vitro* cumulative release of aspirin. (d) Aspirin-enhanced hMSCs proliferation. (*) $p < 0.05$. Results are representative of at least three independent experiments.

rougher than that of the bare PCL scaffold. This indicated successful immobilisation of the liposomes.

3.3. Drug release and cytocompatibility

Fig. 2c presents the cumulative release profiles over 21 days for the aspirin-laden liposomes. A sustained release rate was observed during an initial phase of 5 days. This was followed by a decreasing release rate over the next 5–13 days and a burst release of aspirin at a later period. Overall, the sustained release provided a high concentration of aspirin over the 21 day period. Thus, aspirin release was controlled by encapsulation in the liposome. Notably, a slower but steadier release from the aspirin-laden liposome-decorated substrate was observed in the PS-Asp@Lipo and PCL-Asp@Lipo groups (Fig. 2c and Fig. S3 (ESI†), respectively).

Considering biomedical applications, the cytotoxicity of aspirin-laden liposomes is another critical factor that should be evaluated. The hMSCs were co-cultured with empty liposomes and aspirin-laden liposomes in culture media for 1, 3 and 5 days. The data in Fig. 2d show that all groups exhibited time-dependent cell growth, with ODs increasing with time, indicating that the aspirin-laden liposome-decorated surfaces had good cytocompatibility, thereby allowing normal proliferation of hMSCs. The observed positive effect on cell viability indicates that aspirin-laden liposome-decorated surface could endow substrates with greater cytocompatibility.

3.4. ELISA assay

To evaluate whether our aspirin-laden liposomes retained the anti-inflammatory properties of aspirin, the presence of two major inflammation cytokines (TNF-α and IFN-γ) was evaluated by ELISA after challenging with lipopolysaccharide (LPS). Lipo-polysaccharide, a strong activator of inflammation, induces the production of the above cytokines and additional chemokines,[42] thereby inhibiting osteoblast differentiation in a Myd88-dependent manner.[43–45] To establish an inflammation model in hMSCs, we treated hMSCs with LPS and then examined the expression of inflammatory cytokines in cell culture supernatants. After a 24 h stimulation with LPS, the expression levels of TNF-α and IFN-γ had decreased prominently in the presence of aspirin-laden liposomes (Fig. 3a and b), suggesting that the anti-inflammatory ability of aspirin was preserved in our delivery system.

It has also been reported that aspirin may exert anti-postmenopausal osteoporosis effects in an ovariectomised rat model,[46] indicating its effectiveness for preventing bone loss. Therefore, we examined whether aspirin-laden liposomes could regulate the expression of osteogenic factors in cells by examining OPG and RANKL expression levels in hMSC cultures by ELISA assay. The concentration of RANKL in hMSCs was similar to those observed for TNF-α and IFN-γ (Fig. 3d), but levels of OPG differed significantly (Fig. 3c). The bone protective effect of aspirin seems to be due to the facilitation of stimuli for osteoblast formation, which is indicated by an enhancement in OPG protein levels (Fig. 3c).[46] Conversely, aspirin decreased the RANKL protein levels in bone, resulting in a decrease in stimuli for osteoclast formation. Based on these data, we conclude that the positive effect of aspirin on promoting osteogenic differentiation ability was also preserved in our delivery system, and significantly increased the levels of osteogenic factors while decreasing the levels of inflammatory factors.

3.5. Osteogenic biomarker expression

To further confirm the stimulative effects of aspirin-laden liposomes on osteogenic differentiation in hMSCs, we investigated
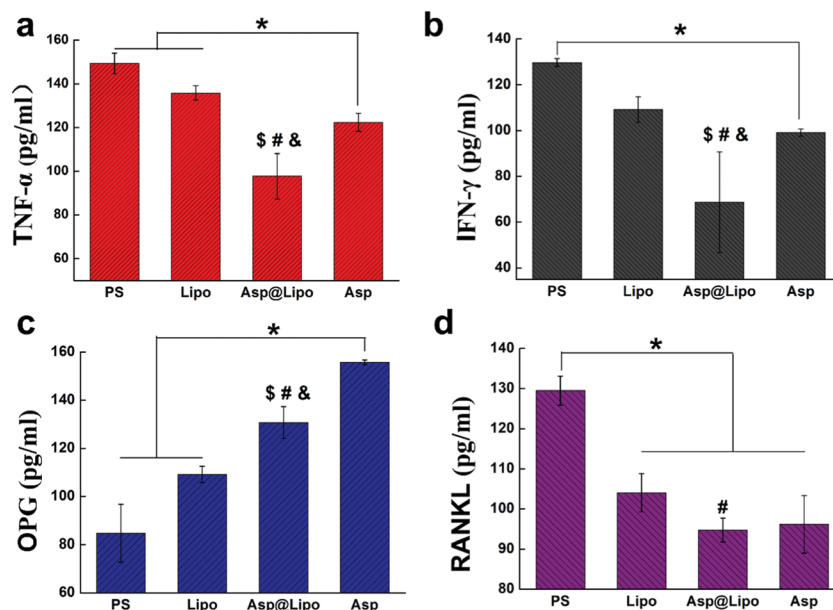

Fig. 3 The effects of our aspirin delivery system on the expression of (a) TNF-α, (b) IFN-γ, (c) OPG, and (d) RANKL. PS, pristine; Lipo, liposomes; Asp@Lipo, aspirin-laden liposomes; Asp, aspirin (75 μg mL^{-1}). \$, #, and & indicate significant differences between the Asp@Lipo and (PS, Lipo, and Asp) groups, respectively (\$, #, &, and *; $p < 0.05$). Results are representative of at least three independent experiments.

624 | J. Mater. Chem. B, 2019, 7, 619–629

This journal is © The Royal Society of Chemistry 2019

the transcription levels of typical osteo-specific genes in hMSCs, such as Runx2, Col1a1, OCN, ALP, OPG and RANKL at 14 days. The hMSCs cultured on PS and surfaces that had been decorated with empty liposomes exhibited lower levels of mRNA corresponding to osteogenic genes. However, hMSCs cultured on surfaces that had been decorated with aspirin-laden liposomes exhibited significantly higher levels of osteogenic gene mRNA levels, presumably due to the sustained release of aspirin. Although aspirin that is dissolved in media, *i.e.* free aspirin, also increases the expression of osteogenic genes, our novel delivery system yielded much higher mRNA levels for Runx2, OCN, Col1a1, ALP and OPG (Fig. 4a–e), but not for RANKL (Fig. 4f). This finding may be attributed to aspirin facilitating Wnt signalling, which is vital for osteoblast formation.[47] On the other hand, aspirin could prevent osteoclast formation by inhibiting the NF-κB pathway, leading to lower levels of RANKL. As shown in Fig. 4e and f, the expression of RANKL in the Asp@Lipo group was the lowest, while that of OPG was the highest, among the groups. These results support the hypothesis that our novel delivery system of aspirin-laden liposomes enhances osteogenic differentiation compared to aspirin alone.

3.6. Alkaline phosphatase (ALP) and matrix mineralisation

Alkaline phosphatase, as an early marker of osteogenesis, was expressed strongly in the osteoblasts.[48] We also assessed ALP expression of hMSCs at 14 days. The data in Fig. 5b show differences in ALP production between the Asp@Lipo group and the PS, Lipo and Asp groups. This indicates that the aspirin-laden liposomes had a stimulative effect on cell differentiation, inducing an up-regulation of ALP, which is correlated to the onset of osteogenic differentiation.

Concomitantly, ARS staining was also performed to evaluate calcium deposition, as an indication of late-stage osteogenesis. As indicated in Fig. 5c and d, similar to the case of ALP activity, more intense red staining was observed in the aspirin-treated groups (Asp@Lipo and Asp) that in the PS and empty liposome groups. Additionally, the formation of a mineralised matrix was more obvious in the Asp@Lipo group than in the Asp group, and hMSCs cultured on Asp@Lipo substrates had the greatest number of calcium nodules (Fig. 5d). These data indicate that the Asp@Lipo delivery system is a better promoter of osteogenic differentiation of hMSCs than aspirin alone.

3.7. Immunofluorescence (IF) analyses

To further explore the osteogenic differentiation of this delivery system, IF analysis was also carried out at 21 days. Strong positive staining of two important osteogenic markers (OCN and OPN) was observed. Higher densities of OCN (green) and OPN (red) were found in the Asp@Lipo group compared with the other samples (Fig. 5e), which is in accordance with our previous (qPCR, ALP and ARS) results. Overall, it demonstrates the high potential of aspirin-laden liposomes for inducing osteogenic differentiation of hMSCs.

3.8. Cytocompatibility of polycaprolactone (PCL) scaffolds

Polycaprolactone is an aliphatic, biocompatible polyester that is inexpensive, nontoxic and flexible.[49] It, has high surface area and interconnected pores, produces 3D structures, and has been widely used in a variety of biomedical applications.[50] The images in Fig. 6a show that PCL scaffolds are suitable for supporting cell growth. The biocompatibility of our PCL scaffolds was evidenced by strong cellular adhesion with spread cell morphologies exhibiting increased proliferation at 3 days. These results provide a basis for the potential application of PCL scaffolds in BTE.
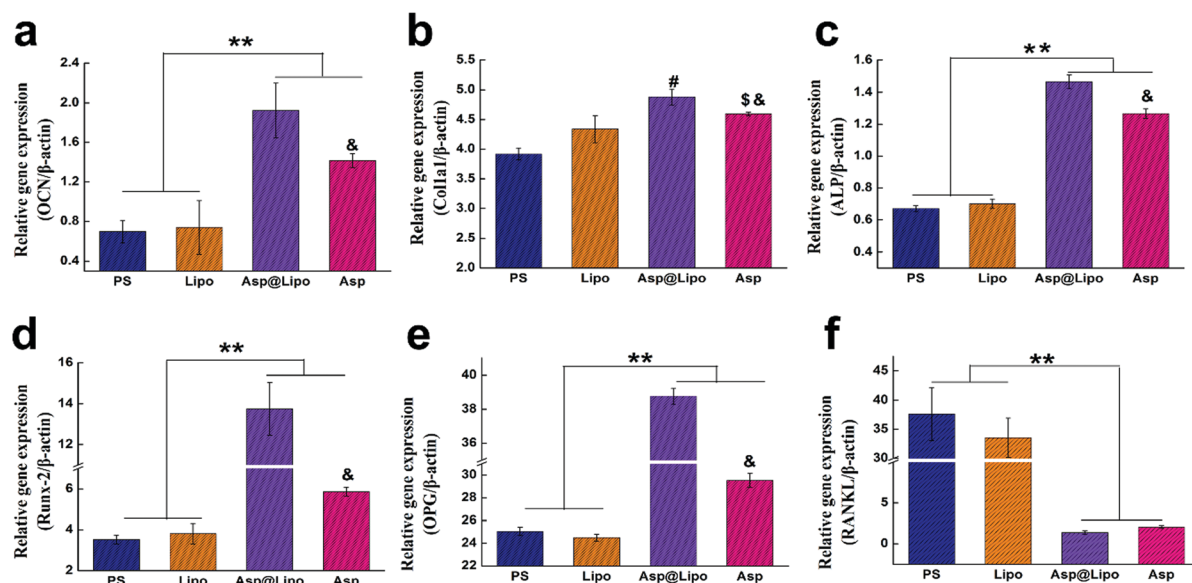

Fig. 4 The effects of our aspirin delivery system on the expression of osteogenic markers by hMSCs on different substrates. (a–f) RT-qPCR analyses of OCN, Col1a1, ALP, Runx-2, OPG, and RANKL expression. # and & indicate significant differences between Asp@Lipo and (PS and Asp) groups, respectively. $ indicates a significant difference between the PS and Asp groups (#, &, $; $p < 0.05$; **, $p < 0.01$). Results are representative of at least three independent experiments.
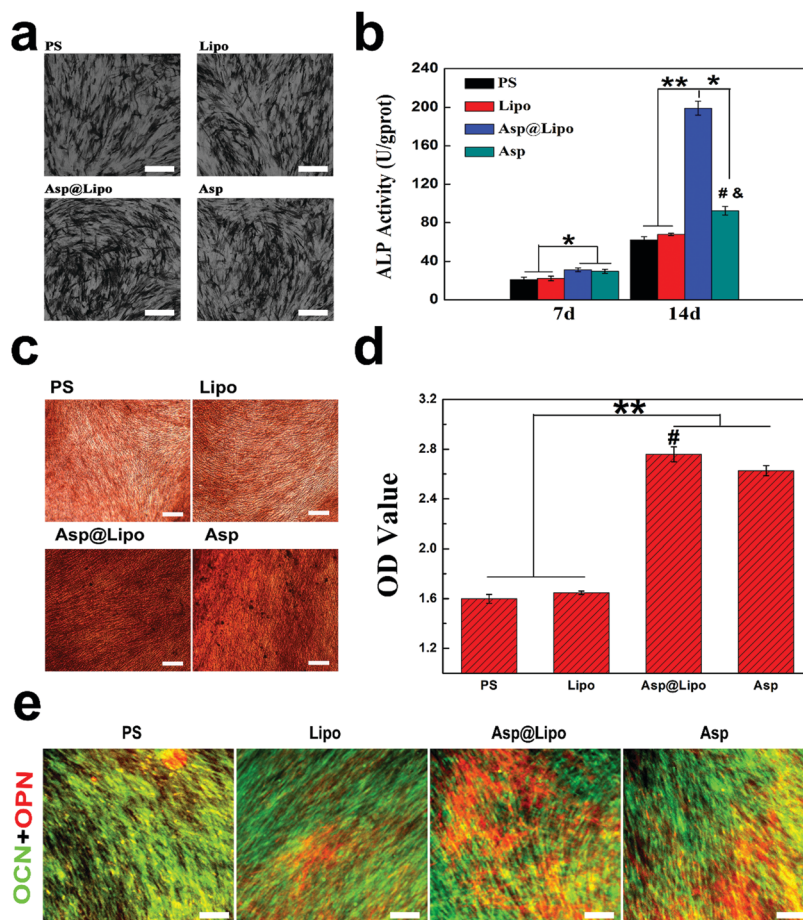
This journal is © The Royal Society of Chemistry 2019

J. Mater. Chem. B, 2019, **7**, 619–629 | 625

Fig. 5 The effects of our aspirin delivery system on osteogenetic by hMSCs on different substrates. (a) Representative image of ALP staining. (b) ALP activity at 7 and 14 days. (c) ARS staining. (d) Calcium deposition at day 21. (e) Representative immunofluorescence images show the distributions of OCN (green) and OPN (red) at day 21. $ significant the differences of Asp@Lipo and Asp groups. $ indicates a significant difference between the Asp@Lipo and Asp groups. # and & indicate significant differences between the Asp and (PS, Lipo) groups, respectively (#, &, $ and *; $p < 0.05$; **, $p < 0.01$). Results are representative of at least three independent experiments. Scale bars indicate 200 μm.

3.9. In vitro osteogenesis ability of PCL-Asp@Lipo

The above results suggest that aspirin-laden liposomes can reduce inflammation of stem cells, and then induce their osteogenic differentiation. As a biocompatible scaffold material, PCL can serve as a good substrate for cell proliferation. Additionally, the ability to control the levels of certain osteogenic factors during cell proliferation on PCL is of great significance in BTE. Therefore, hMSCs were cultured on PCL-Asp@Lipo composite scaffolds. Osteogenesis was induced and cell differentiation was assessed by a series of detection methods. Compared to other groups, hMSCs cultured on PCL-Asp@Lipo composite scaffolds exhibited significantly increased ALP activity at 14 days (Fig. 6b), suggesting enhanced osteogenesis. Mineralisation by ARS staining was consistent with ALP activity, with the empty liposome group yielding the lowest degree of calcium mineralised at 21 days (Fig. 6c). The PCL-Asp@Lipo composite scaffolds yielded a noticeable increase in the mineralised matrix, which became the highest among the groups. Additionally, Fig. 6d shows obviously higher densities of OCN (green) and OPN (red) in the PCL-Asp@Lipo group, in accordance with the results of ALP assays and ARS staining.

All of the above data support our hypothesis that the employment of aspirin-laden liposomes can greatly improve the osteogenic efficiency of hMSCs, with a resulting acceleration in osteogenesis. Furthermore, our findings confirm that PCL-Asp@Lipo composite scaffolds stimulate osteogenic differentiation by enhancing mineralisation, implying that this delivery system possesses potential for application to BTE.

3.10. In vivo osteogenesis ability of PCL-Asp@Lipo

In vivo osteogenesis on hMSC/PCL-scaffold constructs was estimated at 6 weeks after implantation. As shown in Fig. 7a, micro-CT analyses allowed us to visualise the distribution of new bone tissue. The percentage of bone volume was calculated to quantitate the newly formed bone. The data from Fig. 7b show that the bone volume was almost three times higher in the PCL-Asp@Lipo group than in the bare PCL group.

Histological section analyses, including ARS, IHC and IF staining (Fig. 7c), were used to further determine the effects of the implanted composite scaffolds. Histological sections stained with ARS supported the micro-CT analyses and revealed

626 | J. Mater. Chem. B, 2019, 7, 619–629

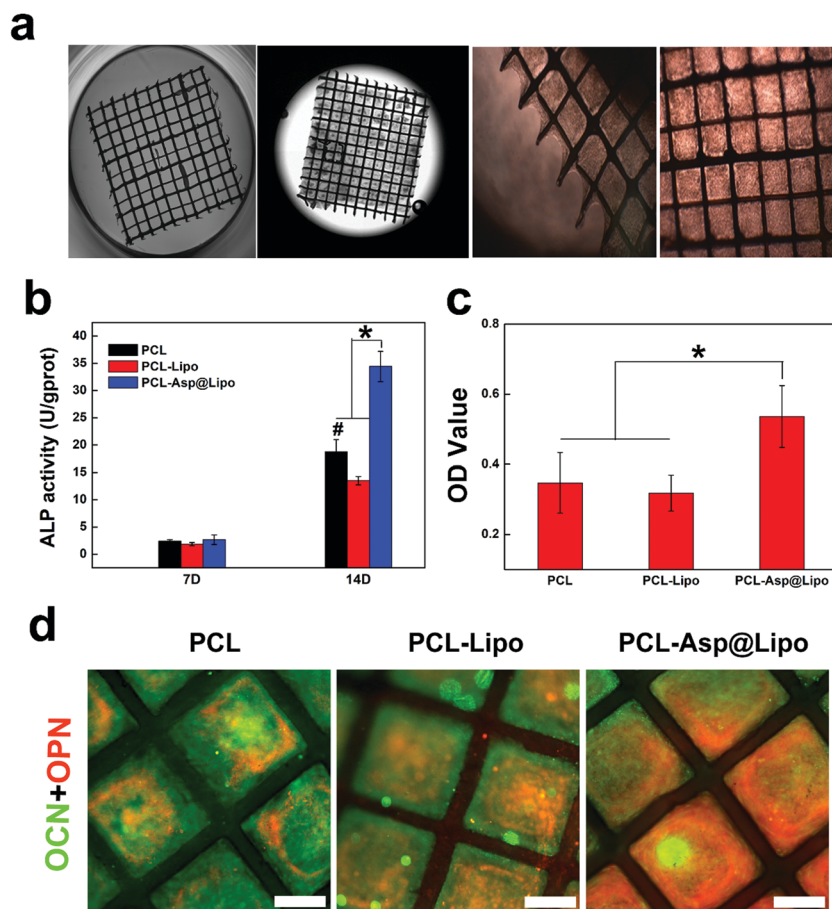This journal is © The Royal Society of Chemistry 2019

Fig. 6 The effects of our aspirin delivery system on the proliferation and osteogenic differentiation of hMSCs on PCL substrates. (a) The morphology of PCL with wide-field and magnified views of PCL surfaces with cells. (b) ALP activity is shown at 7 and 14 days. (c) Calcium deposition is shown at day 21. (d) Representative immunofluorescence images show the distributions of OCN (green) and OPN (red) at day 21. # indicates significant differences between the PCL and PCL-Lipo groups, (# and *; $p < 0.05$). Scale bars indicate 100 μm.

that much more mineralisation occurred in the PCL-Asp@Lipo groups at 6 weeks. A series of immunohistological analyses were also performed to further estimate the *in vivo* osteogenesis of hMSCs-scaffolds. As a bone metabolism marker, OPN expression has widespread application to assess osteogenesis *in vivo*.[51] Compared to the PCL group, IHC-stained sections of the PCL-Asp@Lipo group (Fig. 7c) showed much more significant staining of OPN, which indicates a higher osteogenic ability of the hMSCs/PCL-Asp@Lipo composite scaffold construct. Significantly, both Col1a1 and RUNX-2 were more strongly expressed by hMSCs in the PCL-Asp@Lipo scaffold than by those in the bare PCL group.

Similar to the above *in vitro* results, enhanced *in vivo* osteogenesis of hMSCs cultured on PCL-Asp@Lipo scaffolds was due to the sustained delivery of aspirin. These results confirm that liposome-based delivery of aspirin remarkably enhanced the survivability, proliferation and osteogenic differentiation of hMSCs in the osteogenic niche.

3.11. *In vivo* anti-inflammatory ability of PCL-Asp@Lipo

To estimate the anti-inflammatory effect of hMSC/PCL-scaffold constructs *in vivo*, we investigated the expression levels of

inflammatory factors in a C57BL/6 mouse model with subcutaneous implantation after 3 days. Mice implanted with PCL-Asp@Lipo composite scaffolds exhibited significantly lower concentrations of both TNF-α (Fig. 8a) and IFN-γ (Fig. 8b) compared to those that had been implanted with bare PCL scaffolds ($p < 0.05$), suggesting that our PCL-Asp@Lipo composite scaffolds maintained the anti-inflammation ability of aspirin *in vivo*. This means that conditions can be created for promoting an osteo-inducing effect of hMSCs, as well as late-period bone formation *in vivo*.

4. Conclusions

Bone tissue engineering is an emerging research field that strives to create a local *in vivo* micro-environment suitable for containing cells and drugs in tissue regeneration. One strategy for attaining this goal is the application of biocompatible, cell-seeded scaffolds at the site of the injury or defect,[52] and another approach is to use drug delivery systems for promoting cell-based tissue regeneration.[53] In this study, aspirin-laden liposomes (Asp@Lipo) were successfully integrated into 3D-printed PCL scaffolds with DOPA. The bioactivity of the resulting PCL
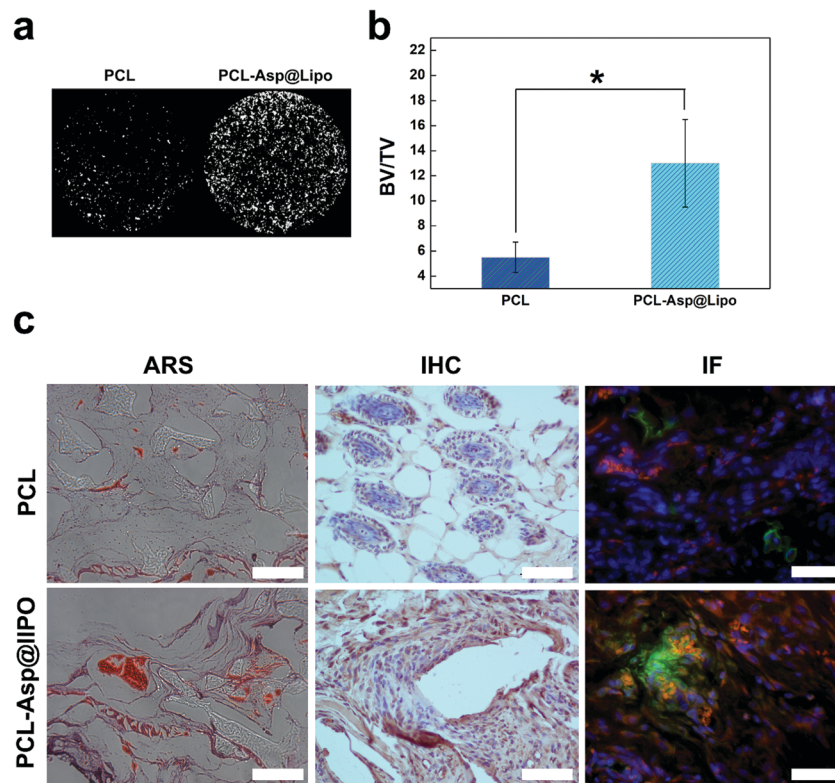
This journal is © The Royal Society of Chemistry 2019

J. Mater. Chem. B, 2019, 7, 619–629 | 627

Fig. 7 *In vivo* mineralization. (a and b) Reconstructed micro-CT images of hMSC-scaffold mineralization and quantitative bone volume after 6 weeks of subcutaneous implantation. (c) Sections of hMSC-scaffolds stained with ARS, IHC (for OPN (brown)), IF (for Col1a1 (red)), RUNX-2 (green), and DAPI (blue) after subcutaneous implantation for 6 weeks. Scale bars indicate 50 μm.
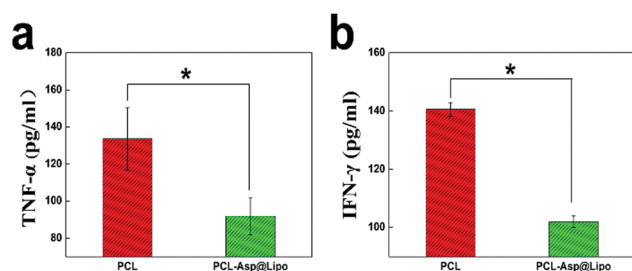

Fig. 8 PCL-Asp@Lipo promoted immunomodulation on subcutaneously implanted composite scaffolds. PCL-Asp@Lipo significantly decreased the concentrations of both (a) TNF-α and (b) IFN-γ compared to the bare PCL group.

scaffold was enhanced due to communication between the aspirin-based delivery system and the scaffold. These novel PCL-Asp@Lipo composite scaffolds enhanced the immunogenicity and differentiation of hMSCs *via* osteo-promoting cellular events and consequently stimulated osteo-inductive processes in a subcutaneous rat model. Our results suggest that a bioactive scaffold with the proposed drug delivery system (Asp@Lipo) can act as a biomimetic substrate for promoting osteo-induction and providing an effective and promising approach for BTE.

Authors' contributions

LY was mainly responsible for designing and performing the experiments, as well as drafting this manuscript. PJJ, LHM, SR, LZY, and LYL played a major role in data analysis of vitro experiments. WH was responsible for the preparation and printing of the scaffold materials. LY, XX, FXM, LQ and BYJ took part in the *vivo* experiments and analyzed the data. WSC and Fuh were mainly participated in the final calibration and publishment.

Conflicts of interest

There are no conflicts to declare.

Acknowledgements

References

1 A. Khademhosseini, J. P. Vacanti and R. Langer, *Sci. Am.*, 2009, **300**, 64–71.

2 A. K. Gaharwar, S. M. Mihaila, A. Swami, A. Patel, S. Sant, R. L. Reis, A. P. Marques, M. E. Gomes and A. Khademhosseini, *Adv. Mater.*, 2013, **25**, 3329–3336.

3 J. Park, I. Y. Kim, M. Patel, H. J. Moon, S.-J. Hwang and B. Jeong, *Adv. Funct. Mater.*, 2015, **25**, 2573–2582.

4 J. M. Grichnik, J. A. Burch, R. D. Schulteis, S. Shan, J. Liu, T. L. Darrow, C. E. Vervaert and H. F. Seigler, *J. Invest. Dermatol.*, 2006, **126**, 142–153.

5 X. Gao, J. Song, Y. Zhang, X. Xu, S. Zhang, P. Ji and S. Wei, *ACS Appl. Mater. Interfaces*, 2016, **8**, 27594–27610.

6 J. R. Vane and R. M. Botting, *Thromb. Res.*, 2003, **110**, 255–258.

7 C. L. Campbell, S. Smyth, G. Montalescot and S. R. Steinhubl, *Jama-Journal of the American Medical Association*, 2007, **297**, 2018–2024.

8 C. M. Turnbull, P. Marcarino, T. A. Sheldrake, L. Lazzarato, C. Cena, R. Fruttero, A. Gasco, S. Fox, I. L. Megson and A. G. Rossi, *J. Inflammation*, 2008, **5**, DOI: 10.1186/1476-9255-5-12.

9 A. Y. Gasparyan, T. Watson and G. Y. H. Lip, *J. Am. Coll. Cardiol.*, 2008, **51**, 1829–1843.

10 H. Sadozai and D. Saeidi, *ISRN Vet. Sci.*, 2013, **2013**, 167521.

11 L. Laine, *Aliment. Pharmacol. Ther.*, 2006, **24**, 897–908.

12 G. T. Noble, J. F. Stefanick, J. D. Ashley, T. Kiziltepe and B. Bilgicer, *Trends Biotechnol.*, 2014, **32**, 32–45.

13 E. Forssen and M. Willis, *Adv. Drug Delivery Rev.*, 1998, **29**, 249–271.

14 P. P. Deshpande, S. Biswas and V. P. Torchilin, *Nanomedicine*, 2013, **8**, 1509–1528.

15 T. Yamaza, Y. Miura, Y. Bi, Y. Liu, K. Akiyama, W. Sonoyama, V. Patel, S. Gutkind, M. Young, S. Gronthos, A. Le, C.-Y. Wang, W. Chen and S. Shi, *PLoS One*, 2008, **3**, DOI: 10.1371/journal.pone.0002615.

16 H. Liu, W. Li, Y. Liu, X. Zhang and Y. Zhou, *Stem Cell Res. Ther.*, 2015, **6**, DOI: 10.1186/s13287-015-0195-x.

17 K.-Y. Chin, *J. Osteoporosis*, 2017, DOI: 10.1155/2017/3710959.

18 M. Nurunnabi, Z. Khatun, K. M. Huh, S. Y. Park, D. Y. Lee, K. J. Cho and Y.-K. Lee, *ACS Nano*, 2013, **7**, 6858–6867.

19 E. V. Paez Espinosa, J. P. Murad and F. T. Khasawneh, *Thrombosis*, 2012, **2012**, 173124.

20 A. D. Bangham and R. W. Horne, *J. Mol. Biol.*, 1964, **8**, 660–668.

21 J. L. Arias, *Expert Opin. Ther. Pat.*, 2013, **23**, 1399–1414.

22 M. Fathi, M. R. Mozafari and M. Mohebbi, *Trends Food Sci. Technol.*, 2012, **23**, 13–27.

23 H. Barani and M. Montazer, *J. Liposome Res.*, 2008, **18**, 249–262.

24 D. Papakostas, F. Rancan, W. Sterry, U. Blume-Peytavi and A. Vogt, *Arch. Dermatol. Res.*, 2011, **303**, 533–550.

25 M. Hasan, N. Belhaj, H. Benachour, M. Barberi-Heyob, C. J. F. Kahn, E. Jabbari, M. Linder and E. Arab-Tehrany, *Int. J. Pharm.*, 2014, **461**, 519–528.

26 M. Takahashi, K.-i. Inafuku, T. Miyagi, H. Oku, K. Wada, T. Imura and D. Kitamoto, *J. Oleo Sci.*, 2006, **56**, 35–42.

27 D. W. Hutmacher, *Biomaterials*, 2000, **21**, 2529–2543.

28 J.-T. Schantz, T.-C. Lim, C. Ning, S. H. Teoh, K. C. Tan, S. C. Wang and D. W. Hutmacher, *Neurosurgery*, 2006, **58**, ONS-E176; discussion ONS-E176.

29 S. W. Low, Y. J. Ng, T. T. Yeo and N. Chou, *Singapore Med. J.*, 2009, **50**, 777–780.

30 X. Wen, K. Wang, Z. Zhao, Y. Zhang, T. Sun, F. Zhang, J. Wu, Y. Fu, Y. Du, L. Zhang, Y. Sun, Y. Liu, K. Ma, H. Liu and Y. Song, *PLoS One*, 2014, **9**, DOI: 10.1371/journal.pone.0106652.

31 X. Xu, L. Wang, Z. Luo, Y. Ni, H. Sun, X. Gao, Y. Li, S. Zhang, Y. Li and S. Wei, *ACS Appl. Mater. Interfaces*, 2017, **9**, 43300–43314.

32 S. He, P. Zhou, L. Wang, X. Xiong, Y. Zhang, Y. Deng and S. Wei, *J. R. Soc., Interface*, 2014, **11**, DOI: 10.1098/rsif.2014.0169.

33 Y. Liu, L. Wang, T. Kikuiri, K. Akiyama, C. Chen, X. Xu, R. Yang, W. Chen, S. Wang and S. Shi, *Nat. Med.*, 2011, **17**, 1594–1601.

34 Y. Li, Z. Luo, X. Xu, Y. Li, S. Zhang, P. Zhou, Y. Sui, M. Wu, E. Luo and S. Wei, *J. Mater. Chem. B*, 2017, **5**, 7153–7163.

35 P. Ramos-Cabrer and F. Campos, *Int. J. Nanomed.*, 2013, **8**, 951–960.

36 Y. Wei, Z. Xue, Y. Ye, Y. Huang and L. Zhao, *Arch. Pharmacal Res.*, 2014, **37**, 728–737.

37 Y. Wei, Z. Xue, Y. Ye, P. Wang, Y. Huang and L. Zhao, *Biomed. Chromatogr.*, 2014, **28**, 204–212.

38 Y. Wei and L. Zhao, *Pharm. Dev. Technol.*, 2014, **19**, 129–136.

39 G. Gregoria, P. D. Leathwoo and B. E. Ryman, *FEBS Lett.*, 1971, **14**, 95–99.

40 S. Jain, S. R. Patil, N. K. Swarnakar and A. K. Agrawal, *Mol. Pharmaceutics*, 2012, **9**, 2626–2635.

41 B. S. Ding, T. Dziubla, V. V. Shuvaev, S. Muro and V. R. Muzykantov, *Mol. Interventions*, 2006, **6**, 98–112.

42 S. L. Tomchuck, K. J. Zwezdaryk, S. B. Coffelt, R. S. Waterman, E. S. Danka and A. B. Scandurro, *Stem Cells*, 2008, **26**, 99–107.

43 K. Bandow, A. Maeda, K. Kakimoto, J. Kusuyama, M. Shamoto, T. Ohnishi and T. Matsuguchi, *Biochem. Biophys. Res. Commun.*, 2010, **402**, 755–761.

44 C. Li, B. Li, Z. Dong, L. Gao, X. He, L. Liao, C. Hu, Q. Wang and Y. Jin, *Stem Cell Res. Ther.*, 2014, **5**, DOI: 10.1186/scrt456.

45 R. E. Shackelford, P. B. Alford, Y. Xue, S. F. Thai, D. O. Adams and S. Pizzo, *Mol. Pharmacol.*, 1997, **52**, 421–429.

46 G. Kaur, M. T. Valarmathi, J. D. Potts, E. Jabbari, T. Sabo-Attwood and Q. Wang, *Biomaterials*, 2010, **31**, 1732–1741.

47 Y. Deng, Y. Sun, X. Chen, P. Zhu and S. Wei, *Mater. Sci. Eng., C*, 2013, **33**, 2905–2913.

48 M. D. Phillips, S. A. Kuznetsov, N. Cherman, K. Park, K. G. Chen, B. N. McClendon, R. S. Hamilton, R. D. G. McKay, J. G. Chenoweth, B. S. Mallon and P. G. Robey, *Stem Cells Transl. Med.*, 2014, **3**, 867–878.

49 S. Ana, R. Erika, H. Arturo, S. Guerrero Sergio, L. Hugo, B.-O. Leticia, S. Lilia, A. Hector, G. de la Puente Silvestre, V. Betha, G. Xochitl and V. Cristina, *Int. J. Morphol.*, 2013, **31**, 321–328.

50 Y. Zhang, N. Cheng, R. Miron, B. Shi and X. Cheng, *Biomaterials*, 2012, **33**, 6698–6708.

51 I. Marcos-Campos, D. Marolt, P. Petridis, S. Bhumiratana, D. Schmidt and G. Vunjak-Novakovic, *Biomaterials*, 2012, **33**, 8329–8342.

52 L. Polo-Corrales, M. Latorre-Esteves and J. E. Ramirez-Vick, *J. Nanosci. Nanotechnol.*, 2014, **14**, 15–56.

53 J. R. Porter, T. T. Ruckh and K. C. Popat, *Biotechnol. Prog.*, 2009, **25**, 1539–1560.

This journal is © The Royal Society of Chemistry 2019

J. Mater. Chem. B, 2019, **7**, 619–629 | 629